

DNA intercalative 4-butylaminopyrimido[4',5':4,5]thieno(2,3-b)quinoline induces cell cycle arrest and apoptosis in leukemia cells

Heggodu G. RohitKumar¹ · Kittur R. Asha¹ · Sathees C. Raghavan² · Gopal M. Advi Rao¹

Received: 27 December 2014 / Accepted: 23 March 2015 / Published online: 29 March 2015
© Springer-Verlag Berlin Heidelberg 2015

Abstract

Purpose DNA intercalators are one of the interesting groups in cancer chemotherapy. The development of novel anticancer small molecule has gained remarkable interest over the last decade. In this study, we synthesized and investigated the ability of a tetracyclic-condensed quinoline compound, 4-butylaminopyrimido[4',5':4,5]thieno(2,3-b)quinoline (BPTQ), to interact with double-stranded DNA and inhibit cancer cell proliferation.

Methods Circular dichroism, topological studies, molecular docking, absorbance, and fluorescence spectral titrations were employed to study the interaction of BPTQ with DNA. Cytotoxicity was studied by performing 3-(4,5-dimethylthiazol-2-yl)-2,5-diphenyltetrazolium bromide (MTT) and lactate dehydrogenase (LDH) assay. Further, cell cycle analysis by flow cytometry, annexin V staining, mitochondrial membrane potential assay, DNA fragmentation, and western blot analysis were used to elucidate the mechanism of action of BPTQ at the cellular level.

Results Spectral, topological, and docking studies confirmed that BPTQ is a typical intercalator of DNA. BPTQ induces dose-dependent inhibitory effect on the proliferation of cancer cells by arresting cells at S and G2/M phase. Further, BPTQ activates the mitochondria-mediated

apoptosis pathway, as explicated by a decrease in mitochondrial membrane potential, increase in the Bax:Bcl-2 ratio, and activation of caspases.

Conclusion These results confirmed that BPTQ is a DNA intercalative anticancer molecule, which could aid in the development of future cancer therapeutic agents.

Keywords DNA intercalators · Chemotherapy · Apoptosis · Leukemia

Introduction

The DNA contained in every mammalian cell is under constant attack by several physical, chemical, and biological agents which may eventually cause mutations. Such extensive genome alteration ranging from a small number of point mutations to widespread aneuploidy in key regulatory genes like proto-oncogenes, tumor suppressor genes, and DNA repair genes leads to cancer [1–3]. Although DNA damage is the principal cause for cancer development, it is also used to treat these malignancies. One of the most effective modalities of cancer therapy includes the use of chemotherapeutic agents that interacts with DNA and targets its associated processes [4, 5]. Research in this area has revealed a range of DNA-recognizing molecules, which include groove binders, alkylating, and intercalator compounds that act as antitumor agents [6]. All these molecules bind to DNA and protein either in reversible or in irreversible manner suggesting the direct relationship between their interaction with macromolecules, hence leading to their therapeutic effects [5, 7]. Therefore, it is of vital interest to study the interaction of small molecules with DNA and their corresponding biological activities in order to understand the mode of drug action.

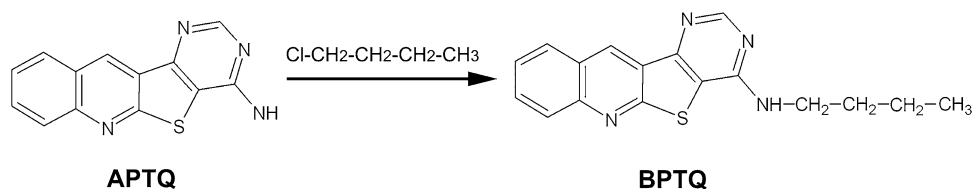
Electronic supplementary material The online version of this article (doi:10.1007/s00280-015-2735-6) contains supplementary material, which is available to authorized users.

✉ Gopal M. Advi Rao
muttagigopal@yahoo.co.in

¹ Department of Biochemistry, Davangere University, Davangere, Karnataka, India

² Department of Biochemistry, Indian Institute of Science, Bangalore, Karnataka, India

Fig. 1 Chemical structure and synthesis of BPTQ



DNA intercalators are mostly polycyclic, aromatic, and planar [8]. As there is an increased need of potential chemotherapeutic molecules, many of the DNA intercalators have been developed and used clinically in cancer therapy, including anthracyclines, mitoxantrone, dactinomycin, and ellipticine. The intercalation of most of these molecules to DNA often leads to the inhibition of topoisomerases, cell cycle arrest, and apoptosis in cancer cells [9–12]. Structure-based design strategies have yielded various planar, aromatic, and heterocyclic molecules with similar physicochemical and biological activities [13, 14]. Quinolines and their derivatives are among such interesting class of molecules, as they have been reported to possess a broad spectrum of biological activities such as antimalarial, antimicrobial [15], and antineoplastic activity [16]. These considerations prompted us to explore a new series of planar heterocyclic quinoline derivatives, pyrimido[4',5':4,5]thieno(2,3-b)quinolines as new cytotoxic anticancer molecules [17, 18].

Earlier in our laboratory, the anticancer activity of 4-aminopyrimido[4',5':4,5]thieno(2,3-b)quinoline (APTQ) was reported [19]. As the APTQ showed good antiproliferative ability, we sought to derivatize APTQ with butylamino functional group in order to develop a more powerful chemotherapeutic molecule. Hence, in search of potent DNA-intercalating anticancer molecules, in this present study, a new representative molecule of pyrimido[4',5':4,5]thieno(2,3-b)quinolines, 4-butylaminopyrimido[4',5':4,5]thieno(2,3-b)quinoline (BPTQ, Fig. 1) was synthesized and analyzed for its ability to recognize DNA and to induce cell death in malignant cells. A detailed investigation of the binding mechanism and biological activity of this molecule revealed that BPTQ effectively intercalates to DNA, arrests cells at S and G2/M phase, and induces mitochondria-mediated apoptosis in tumor cells. This study will be important as there is an increasing need for the development of new and more potent cytotoxic agents to combat cancer.

Materials and methods

Chemicals and reagents

Clostridium perfringens DNA, calf thymus DNA, and poly[d(G-C)] DNA were purchased from Sigma-Aldrich

(USA). DNA solutions were prepared by dissolving the solid material, normally at 1–2 mg/ml, in 50 mM Tris-HCl (pH 7.4), 15 mM NaCl, 1 mM EDTA. The DNA concentrations were determined spectrophotometrically at 260 nm using molar extinction coefficients; *C. perfringens* DNA 12,476 M⁻¹ cm⁻¹, calf thymus DNA 12,824 M⁻¹ cm⁻¹, and poly[d(G-C)] DNA 16,800 M⁻¹ cm⁻¹ [20], and are expressed in terms of base pair equivalents per liter. Fetal bovine serum was from Gibco (USA). Penicillin, streptomycin, annexin V-fluorescein isothiocyanate (FITC) apoptosis detection kit, propidium iodide, and 5,5',6,6'-tetrachloro-1,1',3,3'-tetraethyl benzimidazolcarbocyanine iodide (JC-1) were purchased from Invitrogen (USA). Antibodies were procured from Santa Cruz Biotechnology (USA), Calbiochem (USA), and Invitrogen (USA). All other chemicals unless otherwise mentioned were purchased from Sigma-Aldrich (USA).

Synthesis of BPTQ

Starting material APTQ was synthesized and provided by Dr. S. Y. Ambekar (University of Mysore, Mysore, India) [21]. A mixture of APTQ (0.5 g; 0.002 M) in dimethylformamide (10 ml), anhydrous potassium carbonate (1 g), and butyl chloride (1 ml) was heated under reflux for 3 h. Then, the reaction mixture was filtered and poured into cold water. BPTQ obtained was collected by filtration and recrystallized from aqueous dimethylformamide into clusters. The structural elucidation of the compound was determined by IR and ¹H NMR. The parameters were as follows: BPTQ: C₁₇H₁₆N₄S; IR (Nujol): δ_{max} 3100–3450 and 1664 (N–H) cm⁻¹; ¹H NMR (CF₃COOH): δ 0.95 (3H, *t*, CH₃), 1.2–1.8 (4H, *m*, CH₂-CH₂), 3.95 (2H, *q*, N CH₂), 7.8–8.6 (4H, *m*, H-7, H-8, H-9, H-10), 8.9 (1H, *s*, H-11), 10.1 (1H, *s*, H-2); Anal. calcd. for C₁₇H₁₆N₄S: C, 57.30; H, 4.49; N, 15.73 %; found: C, 56.99; H, 4.31; N, 15.71 %.

Spectroscopy

Absorption, fluorescence, and circular dichroism spectroscopy were employed to study the binding ability of the BPTQ with DNA. Loss of BPTQ from solution was minimized by wetting BPTQ in a small volume of concentrated HCl and further diluting with 50 mM Tris-HCl (pH 7.4), 15 mM NaCl, 1 mM EDTA. The final concentration of HCl in working solution

was <0.005 N. Since a number of drugs have been reported to exhibit sequence specificity in binding to DNA, interaction of BPTQ with *C. perfringens* DNA (28 % GC), calf thymus DNA (42 % GC), and poly[d(G-C)] DNA (100 % GC) was analyzed.

BPTQ (81 μ M) was incubated with various concentrations of *C. perfringens* DNA, calf thymus DNA, and poly[d(G-C)] DNA in 50 mM Tris-HCl (pH 7.4), 15 mM NaCl, 1 mM EDTA. The absorbance and fluorescence emission spectrum of BPTQ on addition of each DNA aliquot was recorded with Spekol spectrophotometer (Analytic Jena, Germany) and F-2000 fluorescence spectrophotometer (Hitachi, Japan), respectively. BPTQ solutions with or without DNA were excited at 288 nm, and fluorescence intensities were monitored at 446 nm. The association constants and stoichiometries of the hydrogen-bonding interactions in the BPTQ-DNA systems were determined by plotting double reciprocal plot of the change in absorbance or fluorescence of BPTQ as a function of DNA concentration by the method of Benesi and Hildebrand [22, 23].

Circular dichroism (CD) spectra were recorded at 25 °C on Jasco-20 dichrograph (Jasco International Co, Ltd, Japan). Spectra of calf thymus DNA solution (54.58 μ M) in 50 mM Tris-HCl (pH 7.4), 15 mM NaCl, 1 mM EDTA, in the absence and presence of various concentrations of BPTQ (0–130 μ M), were scanned in 10-mm quartz cuvette. Measurements were taken over the spectral range 240–325 nm. Three spectra were acquired and averaged for each sample.

Melting temperature studies

Thermal denaturing studies were performed using calf thymus (16.374 μ M) DNA with BPTQ (81 μ M). The increase in the absorbance at 260 nm, corresponding to the transition from the double-strand to single-strand DNA, was used to monitor the thermal denaturation of DNA [24].

Gel mobility shift assay

Intercalation assay was performed as described previously [25]. Briefly, 100 ng of supercoiled pUC19 was incubated with 100 μ M ethidium bromide or increasing concentrations of BPTQ (10, 50, 100, and 250 μ M) for 30 min at room temperature. Electrophoretic assays were run using a 1.5 % agarose gel without ethidium bromide at 90 V for 2 h in $0.5 \times$ Tris-borate-EDTA buffer. The gels were then stained with ethidium bromide (0.5 μ g/ml), destained, and visualized under ultraviolet (UV) light.

Molecular docking of BPTQ-DNA complex

For in silico molecular docking, ligand–nucleic acid complex crystal structure for ellipticine was obtained

from the Protein Data Bank (PDB: 1Z3F). The structure was solved by molecular replacement using the DNA coordinates of the d(CGTACG)₂-ellipticine structure [26] as a starting model. BPTQ was docked to the double-helix DNA fragment d(CGTACG)₂ using the Hex 6.3 program, an interactive protein docking and molecular superposition program, which support a Fourier-based calculation of electrostatic interaction energies [27]. The orientations were scored using shape and electrostatic correlations with default docking control values ($n = 25$). The best 2000 of the $n = 25$ orientations were then refined using a soft molecular mechanics rigid body minimization algorithm. After minimization, the lowest energy solution was selected from all docking solutions. Ellipticine was used as a reference molecule for comparison.

Cell lines and culture

Human promyelocytic leukemia (HL-60), acute lymphoblastic leukemia (MOLT-4), breast adenocarcinoma (MCF7), colon adenocarcinoma (COLO 205), kidney carcinoma (A-498), mouse melanoma (B16-F10), and normal human embryonic kidney (293T) cells were obtained from National Centre for Cell Science, Pune, India. Human B cell precursor leukemia (NALM-6) and acute lymphocytic leukemia (Reh) cell lines were kindly provided by Dr. M. Lieber (USA). HL-60, MOLT-4, NALM-6, Reh, and COLO 205 were routinely maintained and grown in RPMI-1640 supplemented with 10 % heat-inactivated FBS, L-glutamate (2 mM), penicillin (100 IU/ml), and streptomycin (100 μ g/ml) at 37 °C in a humidified atmosphere containing 5 % CO₂. MCF7 and A-498 were maintained in Eagle's minimum essential medium. B16-F10 and 293T were maintained in Dulbecco's modified Eagle's medium. Cell integrity was assessed by trypan blue exclusion assay. 50 mM stock of BPTQ was prepared in dimethylsulfoxide (DMSO) and diluted with respective media to give final concentrations. Final solvent concentration in cell culture was less than 0.1 % (v/v), which had no effect in any of the parameters studied. In all experiments, DMSO-treated cells were used as control.

MTT assay

Cytotoxicity of the BPTQ was assessed using the 3-(4,5-dimethylthiazol-2-yl)-2,5-diphenyltetrazolium bromide (MTT) assay [28]. Briefly, exponentially growing cells were seeded in 96-well culture plates with various drug concentrations in a volume of 100 μ l. After 48 h of incubation at 37 °C, MTT was added and cell viability was

quantified using a Bio-Rad (USA) microplate reader. IC_{50} values were calculated.

LDH release assay

Release of lactate dehydrogenase (LDH) is an indicator of loss of membrane integrity and hence cell injury. LDH assay was performed to assess its release into the medium following treatment (1, 5, 10, 25, and 50 μ M) on MOLT-4 cells for 24, 48, and 72 h using standard protocols [29]. The percentage of LDH released was calculated as follows: (LDH activity in media)/(LDH activity in media + intracellular LDH activity) \times 100.

Cell cycle analysis by flow cytometry

Effect of BPTQ on cell cycle distribution was analyzed as described previously [3]. MOLT-4 cells were grown at a density of 1×10^6 cells in 100-mm culture dishes and were treated with BPTQ (0.5, 1, 5, and 10 μ M) for 48 h. Cells were then harvested, washed, fixed overnight in 70 % ethanol at -20 °C before being washed, digested with RNase A, stained with propidium iodide (50 μ g/ml), and analyzed by flow cytometry using Cell Quest Pro software (FACS-Calibur, Becton–Dickinson).

Quantification of apoptosis by flow cytometry and confocal imaging

The annexin V labeling assay was performed by using annexin V-FITC apoptosis detection kit (Invitrogen, USA) as per manufacturer's instruction. Briefly, MOLT-4 cells were incubated in 1 and 5 μ M BPTQ for 48 h and stained with fluorescein isothiocyanate-conjugated annexin V and propidium iodide. The stained cells were incubated for 15 min at 37 °C, analyzed in flow cytometer, and imaged by laser-scanning confocal microscopy (LSM 510 META; Zeiss).

Mitochondrial membrane potential measurement

Mitochondrial membrane potential was measured using fluorescent potentiometric dye JC-1 as described previously [17]. MOLT-4 cells were treated with BPTQ (5 μ M) for different time intervals and then washed and labeled for 45 min with 10 μ M JC-1 at 37 °C. Cells were washed three times, resuspended in PBS, and fluorescence was measured. Subsequently, the changes in fluorescence were monitored at two different wavelengths as mentioned above. The ratio of the reading at 590 nm (red fluorescence of JC-1 aggregates) to 530 nm (green fluorescence of diluted JC-1) (590: 530 nm ratio) was considered as the relative $\Delta\Psi_m$ value.

Fig. 2 BPTQ binds to DNA through intercalation. **a–d** UV–visible and fluorometric spectral analysis of BPTQ interaction with DNA. Spectrophotometric and fluorometric titrations were performed by the addition of increasing aliquots of *C. perfringens* DNA, calf thymus DNA, and poly[d(G-C)] DNA solutions to BPTQ and scanning the UV–visible and fluorescence spectrum (excitation wavelength, 288 nm; emission wavelength, 446 nm) after each addition. **a–c** Were the UV–visible spectra of BPTQ in the absence and presence of *C. perfringens* DNA, calf thymus DNA, and poly[d(G-C)] DNA, respectively. **d** Fluorescence emission spectra of BPTQ in the absence and presence of calf thymus DNA. See also Supporting Information. **e** Stereoviews of the BPTQ–DNA docking complexes. *Upper panel*, The intercalated d(CGATCG)₂ hexanucleotide. *Middle panel*, Projection down the helix axis of a d(CGATCG)₂ hexanucleotide with the sandwiched ligand. *Lower panel*, Space-filling model of intercalated complex. *Left panel*, BPTQ; *Right panel*, Ellipticine. **f** CD spectra of calf thymus DNA titrated with (1) 0 μ M, (2) 32.50 μ M, (3) 65.00 μ M, (4) 97.50 μ M, (5) 130.00 μ M, and (6) 162.50 μ M BPTQ. **g** Effect of BPTQ on the electrophoretic mobility of supercoiled DNA. Supercoiled DNA was pre-incubated with increasing concentrations of BPTQ for 30 min and subjected to electrophoresis in 1 % agarose gel. S, plasmid DNA; EB, ethidium bromide; M, molecular weight ladder

Caspase-3 activity

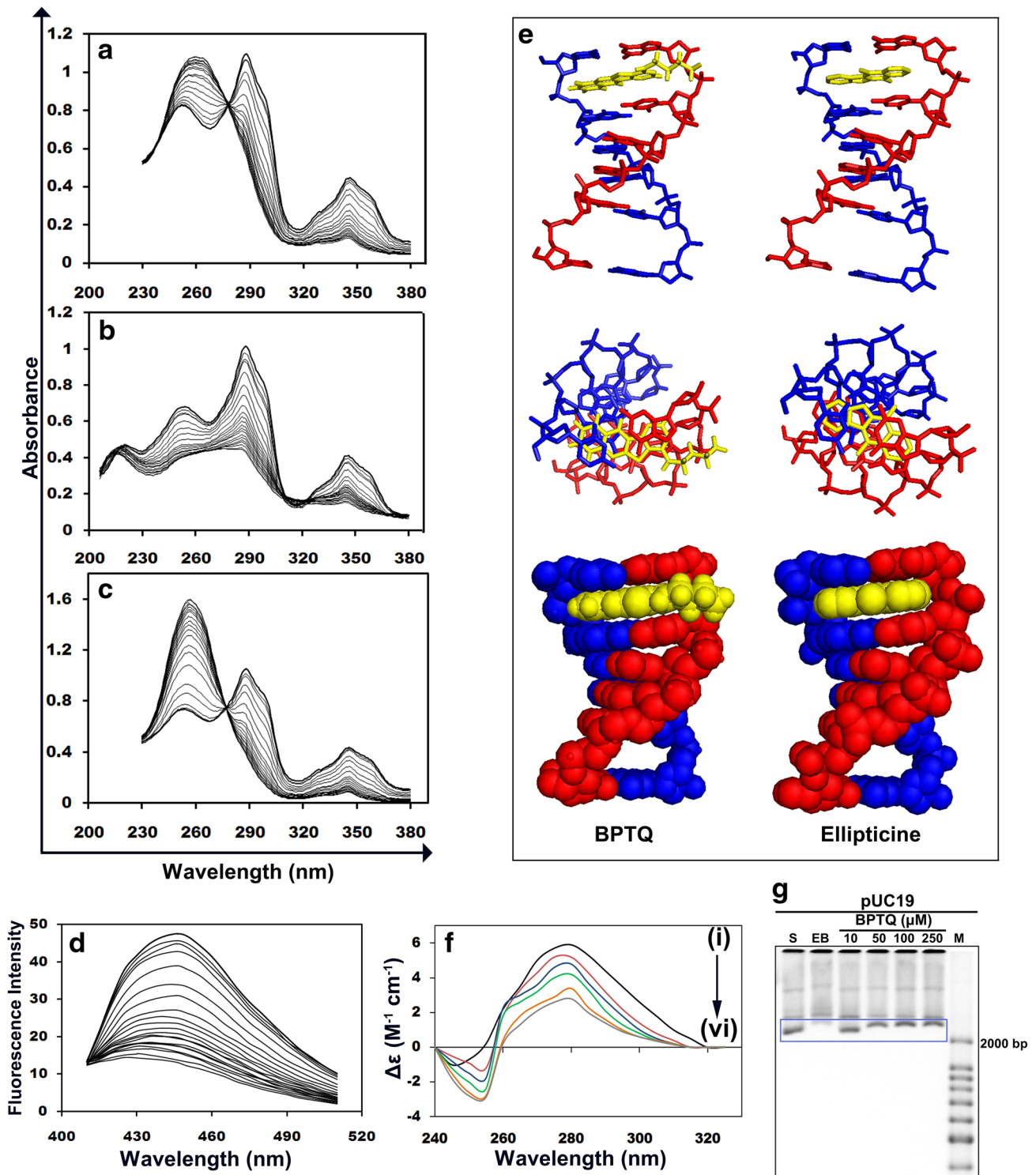
Caspase-3 assay was performed in MOLT-4 cells using caspase-3 colorimetric assay kit (Sigma, USA) following the manufacturer's suggested protocol. The caspase activity was represented as the concentration of p-nitroanilide (pNA) formed per min per ml of cell lysate.

DNA fragmentation

Apoptosis was demonstrated by DNA fragmentation. MOLT-4 cells were treated with BPTQ (5 and 10 μ M) for 48 h. After incubation, both treated and untreated cells were collected, and cytosolic DNA was prepared. DNA was then analyzed on 1.5 % agarose gel by electrophoresis as previously described [30].

Western blot analysis

To determine the levels of protein expression, MOLT-4 cells were treated with BPTQ (1, 5, and 10 μ M) for 48 h and whole-cell extracts were prepared as described previously [31]. The proteins were resolved over 8–10 % SDS-polyacrylamide gel electrophoresis. After electrophoresis, the proteins were electrotransferred onto PVDF membranes (Millipore, India), blotted with each antibody, and detected by chemiluminescent solution (Immobilon western, Millipore, India) in a gel documentation system (LAS 3000, FUJI, JAPAN). Primary antibodies against Bcl-2, Bax, p53, β -actin (Invitrogen, USA), caspase-8, caspase-9, BID (Santa Cruz Biotechnology, USA), and PARP (Calbiochem, USA) were used for the current study.



Statistical analysis

All assays were performed in triplicate. Statistical analysis of the data was performed by using Student's *t* test, one- or two-way analysis of variance. Significance was established upon a $p < 0.05$.

Results

Synthesis

The spectral data support the structure of BPTQ. IR spectrum shows an absorption broadband between 3100 and 3450 cm^{-1}

and medium sharp band at 1664 cm^{-1} characteristic of quino-line and NH group. The ^1H NMR spectrum of BPTQ showed the appearance of new signal due to butyl protons. The structure of the rearranged product was confirmed by its synthesis.

BPTQ binds to DNA through intercalation

Different spectroscopic methods were used to study the interaction of BPTQ with DNA. UV–visible spectrum of BPTQ was characterized by three maxima at 244, 288, and 341 nm. Figure 2a, b, and c shows the absorption spectra of BPTQ in the absence and presence of *C. perfringens* DNA, calf thymus DNA, and poly[d(G-C)] DNA, respectively. The addition of increasingly higher concentration of DNA led to hypochromic changes in its visible absorption spectra, as a result of the formation of more stable complexes. The extent of hypochromism in BPTQ absorption of about 60 %, as the composite band at 288 nm, was higher with poly[d(G-C)] DNA compared to calf thymus DNA (58 %) and *C. perfringens* DNA (50 %). A clear, single isosbestic point was observed for each DNA (at 278 nm for poly[d(G-C)] DNA and *C. perfringens* DNA, at 309 nm for calf thymus DNA) which suggests that BPTQ and DNA were related linearly by stoichiometry. These spectral characteristics may suggest a binding mode, involving intercalative interaction between the drug chromophore and the DNA base pairs. The 1:1 and 1:2 Benesi–Hildebrand methods were used to investigate the association constants and stoichiometries of the interactions in the two systems [22, 23]. 1:1 and 1:2 (See Supplementary Material, Fig. A1) plots of a set of experimental data of the BPTQ–DNA system showed that the linear fit of 1:1 Benesi–Hildebrand plot (with a correlation coefficient $R^2 > 0.99$) was more than the linear fit of 1:2 Benesi–Hildebrand plot for all three DNA tested, suggesting that interaction pair was more likely in the 1:1 form. The association constant (K_a) of the BPTQ with *C. perfringens* DNA, calf thymus DNA, and poly[d(G-C)] DNA was calculated to be 0.558×10^4 , 1.289×10^4 , and $1.466 \times 10^4\text{ M}^{-1}$, respectively.

DNA-binding constants were also determined by fluorescence spectroscopy. The optimal excitation and emission wavelength for BPTQ were, respectively, 288 and 446 nm. Fluorescence of BPTQ was quenched significantly (72 % hypochromism) upon increasing addition of calf thymus DNA and a classical shift in the emission peak (about 16 nm) toward lower wavelength occurred (Fig. 2d). The intrinsic binding constant of $0.819 \times 10^4\text{ M}^{-1}$ was obtained, confirming the result obtained in the UV–visible spectral study. These spectral measurements indicate that BPTQ binds to DNA.

To test whether BPTQ intercalated into DNA, DNA melting analysis was performed, as the intercalation of small molecules into the double-helix is known to increase the T_m of DNA. The extinction coefficient of DNA bases at

260 nm in the double-helix form is much less than that of the single-stranded form; hence, melting of the helix leads to an increase in the absorbance at 260 nm [32, 33]. The DNA melting study was carried out with calf thymus DNA in the absence and presence of BPTQ. The T_m for calf thymus DNA without ligand was $65\text{ }^\circ\text{C}$, and with BPTQ, a single transition at $70\text{ }^\circ\text{C}$ was observed. Hence, it is evident that the binding of BPTQ to DNA was through intercalation.

It is also known that the intercalation of some linear or flat aromatic molecules into the double-stranded polynucleotides induces large chirality changes and consequently significant effect in their CD spectra [34]. The CD spectrum of free calf thymus DNA exhibits a positive absorption band at 280 nm and a negative band at 245 nm, characteristic of the B-form of DNA. The positive and negative bands were, respectively, due to base stacking and helicity of the DNA [35]. Figure 2f shows the induced structural changes of DNA by the addition of BPTQ in terms of the molar ellipticity. Upon increasing addition of BPTQ, the negative peak showed the decrease in the molar ellipticity and was shifted from 245 to 255 nm. The positive peak also decreased gradually. Such changes in CD spectra reflect the distortion in the helical nature of B-DNA. Drug–base stacking and the dipole–dipole interactions stabilizing the intercalated drug in the helix resulted in the shift of peak to a larger wavelength (and hypochromism) of the chromophore transition [20, 35].

Strong evidence for the intercalative binding of BPTQ to the double-helix DNA was obtained from gel mobility shift assay, by observing changes in the mobility of supercoiled DNA upon BPTQ treatment. The mobility of supercoiled plasmid DNA was retarded dose dependently with BPTQ addition (Fig. 2g). Ethidium bromide served as positive control.

The computational docking analysis provided further evidence that BPTQ intercalates into DNA. Comparison of the binding orientation of the BPTQ molecule with the ellipticine revealed that the BPTQ exhibited similar orientation as that of ellipticine molecule. BPTQ has a strong preference for the d(GpC)–d(CpG) site as they intercalated in d(GpC)–d(CpG) site, and no BPTQ molecules are inserted in the d(ApT)–d(TpA) site (Fig. 2e). Ellipticine was also earlier reported to possess similar d(GpC)–d(CpG) preference [26]. The qualitative analysis of the docked models was based on the lowest energy poses for molecule. BPTQ–d(CGTACG)₂ docking models showed lower docking energy (-372.5) than that of ellipticine–d(CGTACG)₂ (-351.2) suggesting that BPTQ is a potent DNA intercalator.

BPTQ induces cytotoxicity in cancer cells

To study the cytotoxic effect of BPTQ, MTT assay was performed upon various cancer cell lines derived from leukemia

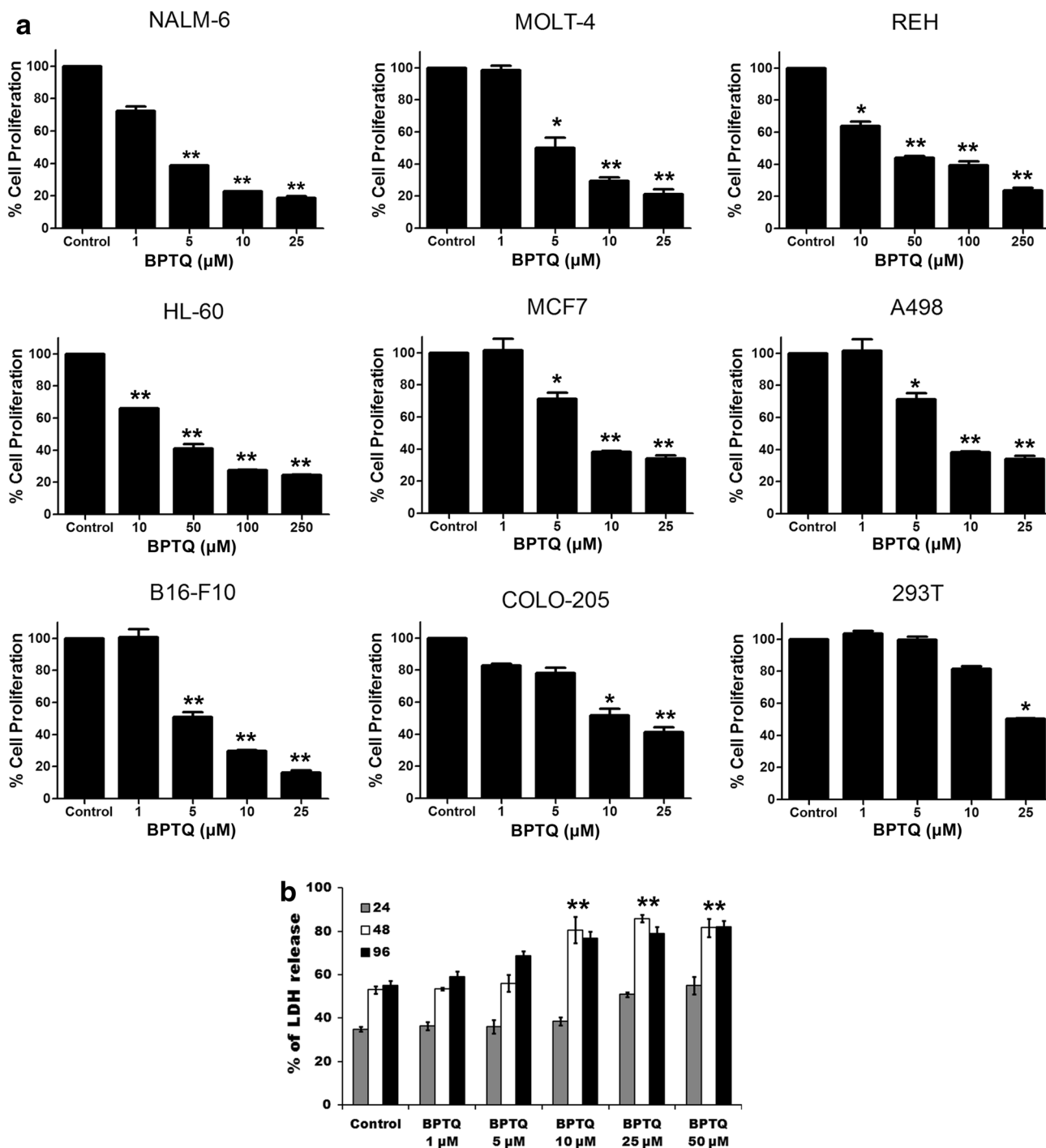


Fig. 3 Evaluation of cytotoxicity of BPTQ on different cancer cells. **a** Bar diagrams showing comparison of cytotoxicity of BPTQ on cancer cell lines. Different cancer cells were incubated with different concentrations of BPTQ for 48 h, and cell viability was determined by MTT assay. DMSO served as vehicle control. **b** Cytotoxicity measured as LDH release upon BPTQ treatment. MOLT-4 cells

were treated with different concentrations of BPTQ for 24, 48, and 72 h. Percentage of LDH released from cells to medium was analyzed in both treated and untreated cells. In all panels, the data are representative of three independent experiments. Mean ± SEM are shown (**p* < 0.05, ***p* < 0.01)

(MOLT-4, Reh, HL-60, and NALM-6), breast (MCF7), colon (COLO 205), kidney (A-498), and mouse melanoma (B16-F10). Results showed that treatment with BPTQ

significantly decreased the proliferation of all the cancer cell lines tested in a dose-dependent manner (Fig. 3a). The IC₅₀ values were in the range of 0.5–17 μM, with leukemia

Table 1 IC₅₀ values of BPTQ against various cancer cell lines

Cancer type	Cell line	BPTQ (μM)	Ellipticine (μM)
Acute lymphoblastic leukemia	MOLT-4	2.05 ± 0.80	0.38 ± 0.07
Pre-B cell leukemia	NALM-6	1.98 ± 0.02	ND
Promyelocytic leukemia	HL-60	12.07 ± 0.52	1.12 ± 0.20
Acute lymphocytic leukemia	Reh	10.04 ± 3.18	ND
Colon adenocarcinoma	COLO-205	16.61 ± 3.82	0.97 ± 0.11
Breast adenocarcinoma	MCF7	4.30 ± 0.70	1.86 ± 0.22
Kidney carcinoma	A498	15.54 ± 2.90	ND
Mouse melanoma	B16-F10	2.72 ± 0.50	1.32 ± 0.13

IC₅₀ values were calculated from the results of the MTT assays by nonlinear regression of the dose–log response curves. Mean ± SEM are shown

ND not determined

cells appeared to be the most sensitive among the panel of cell lines evaluated (Table 1). Therefore, further studies were continued using MOLT-4 cells to elucidate the mechanism of cell death induction by BPTQ. Interestingly, BPTQ induced only limited cytotoxicity in normal cell line, 293T, compared to cancer cell lines studied (Fig. 3a).

Further cytotoxicity was also confirmed by estimating the release of the LDH enzyme from cells. Lower concentrations of BPTQ did not induce the release of LDH. Nevertheless, BPTQ increased the release of LDH from MOLT-4 cells at concentrations of 25 and 50 μM (Fig. 3b), suggesting cytolysis at only higher concentrations of BPTQ treatment.

BPTQ induces S phase arrest and apoptosis in MOLT-4 cells

Flow cytometry was used to investigate whether the inhibition of MOLT-4 proliferation by BPTQ was mediated by regulating cell cycle progression (Fig. 4a). MOLT-4 cells showed the typical cell cycle distribution with 53 % cells in G0/G1 phase, 29 % cells in S phase, and 11 % cells in G2/M phase (Fig. 4b). Dose response effect of BPTQ was analyzed at 48 h of treatment. It is interesting to observe that, when MOLT-4 cells were treated with 5 μM BPTQ, the population of cells in S phase was significantly increased to 63 %, with a slight increase in G2 M cell population (17 %, Fig. 4c, d). Accumulation of cells in G2/M phase was further increased in 10 μM treatment (32 %). Meanwhile, the proportion of cells in G0/G1 was greatly reduced (Fig. 4b). These observations clearly indicate that the BPTQ arrests cell progression at S and G2/M phase.

Cell cycle arrest often leads to the initiation of apoptosis. To identify the mechanism of cell death induced by

BPTQ, annexin V-FITC and propidium iodide double staining were performed. Treatment with 1 μM BPTQ resulted in the increase of apoptotic cell population to 23 %, which further increased dose dependently to 36 % when treated at 5 μM (Fig. 4e, f). The necrotic cell population was very negligible. Confocal imaging of stained cells also supports the result of flow cytometry. Cells treated with BPTQ were stained with either by annexin V-FITC alone (early apoptosis) or by both annexin V-FITC and propidium iodide dyes (late apoptosis) (Fig. 4g). Untreated cells did not show any of the fluorescence, substantiating the mode of cell death induced by BPTQ was by apoptosis.

BPTQ induces apoptosis through the intrinsic mitochondrial pathway

Mitochondria have been shown to play a major role in apoptosis. Depolarization of mitochondrial membrane potential ($\Delta\Psi_m$) was known to be an initial step in mitochondria-mediated cell death. The JC-1 dye was used to monitor $\Delta\Psi_m$ upon addition of BPTQ to MOLT-4 cells, estimated as the 590:530 nm emission ratio. A marked fall in the membrane potential was observed following 5 μM BPTQ treatment ($p < 0.01$, Fig. 5a). The drop in potential started at about 6 h and continued as time lapsed. Pre-incubation with 50 μM of N-acetyl-L-cysteine did not reverse the fall in $\Delta\Psi_m$, ruling out the role of reactive oxygen species in the collapse of $\Delta\Psi_m$.

Downstream of mitochondrial membrane potential disruption, caspase activation is an essential event in the execution of apoptosis [36]. To investigate the induction of apoptosis by BPTQ, colorimetric substrate of caspase-3 was used. Results showed that 5 μM BPTQ has significantly increased the intracellular caspase-3 activity compared to control ($p < 0.01$). The increase in the caspase-3 activity was about fivefold to that of control and was reversed when caspase-3-specific inhibitor (acetyl-Asp-Glu-Val-Asp-al) was added (Fig. 5c). This confirms that the observed activity was by caspase-3 and not by other non-caspase proteases. Therefore, it is proved that BPTQ induces caspase-dependent apoptosis in leukemia cells.

Further to elucidate the mode of apoptosis, the expression levels of apoptosis-regulating proteins following BPTQ treatment were studied (Fig. 5b). As MOLT-4 cells were sensitive to BPTQ, they were selected for this study. The Bcl-2 family proteins are known to be the major regulator of apoptosis [37]; hence, the ratio of Bax:Bcl-2 was determined upon treatment of BPTQ. Results showed that BPTQ led to a remarkable increase in the Bax:Bcl-2 ratio by an increase in Bax (proapoptotic) and decrease in Bcl-2 (antiapoptotic) level, particularly at 1 and 5 μM concentrations. BID expression was also decreased upon treatment,

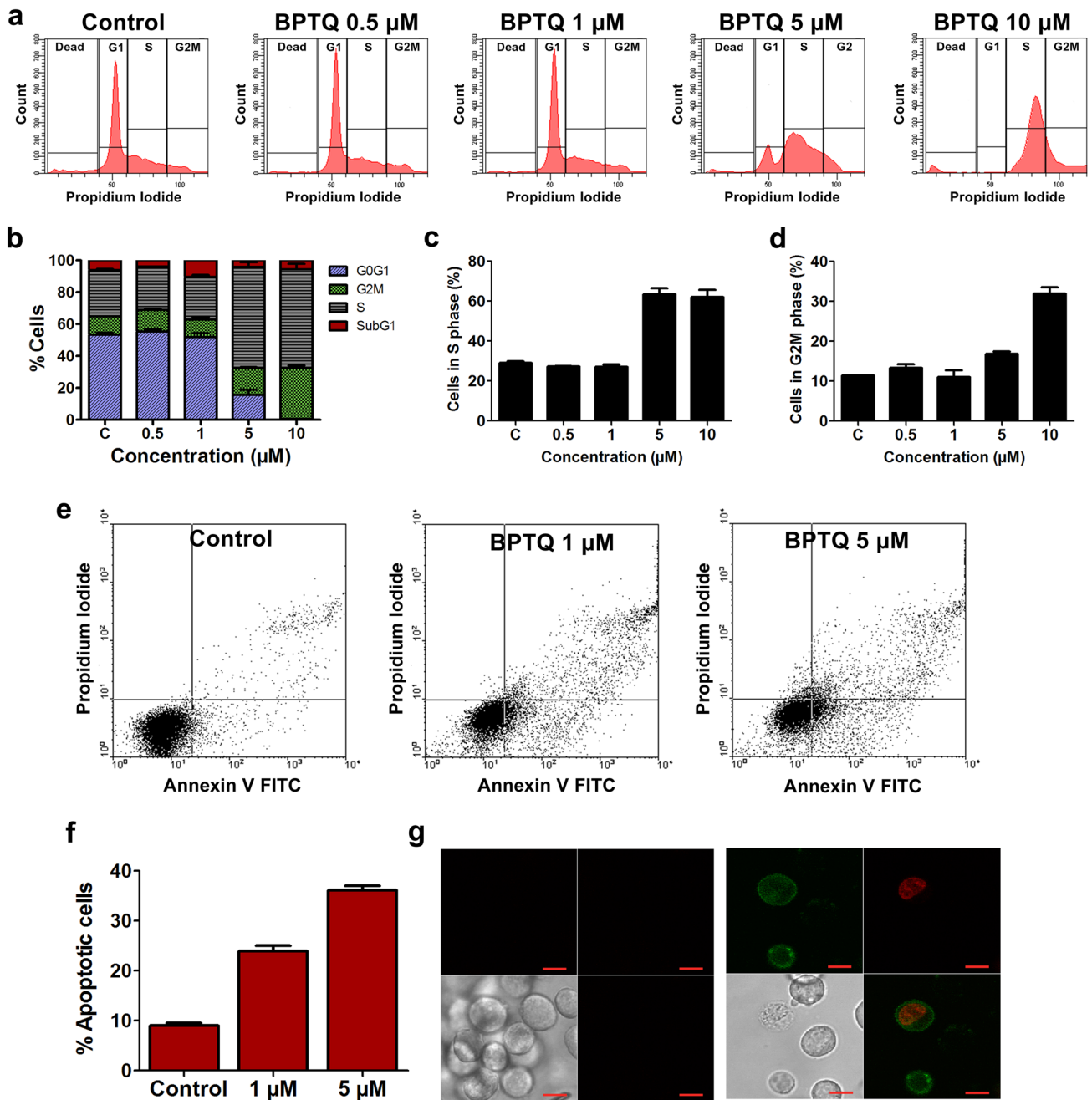


Fig. 4 BPTQ induces cell cycle arrest and apoptosis in leukemia cells. **a** BPTQ blocks cell cycle progression at S and G2/M phase. MOLT-4 cells were exposed to 0.5, 1, 5, and 10 μM BPTQ for 48 h and then processed as described under “Materials and methods” section. Cells were then stained with propidium iodide and analyzed using flow cytometry. Representative histograms are shown. **b–d** Data from (a) represented by bar chart. **e** BPTQ induces apoptosis in leukemia cells. MOLT-4 cells were exposed to 1 and 5 μM of BPTQ for 48 h, labeled with annexin V-FITC and propidium iodide as detailed under “Materials and methods” section. Cells were ana-

lyzed by flow cytometry. Representative dot plots are shown. **f** Data from (e) represented by bar chart. **g** Visualization of annexin V-FITC/propidium iodide stained cells by confocal microscopy. *Left panel*, Untreated cells did not show fluorescence, and in the bright field image, the integrity of the cells was observed; *Right panel*, Cells treated with BPTQ were stained with either by annexin V-FITC alone (early apoptosis) or by both annexin V-FITC and propidium iodide dye (late apoptosis). Scale bar, 10 μm . In (b, c, d, and f), data shown are from minimum of two independent experiments. Bar graph shows mean \pm SEM

indicating its cleavage and conversion to proapoptotic tBID. This indicates that cells were committed to apoptosis via the mitochondrial pathway. Since p53 is a known

activator of Bcl-2 family proteins, expression levels of p53 were tested. A similar increase in the p53 expression was noted in BPTQ-treated cells.

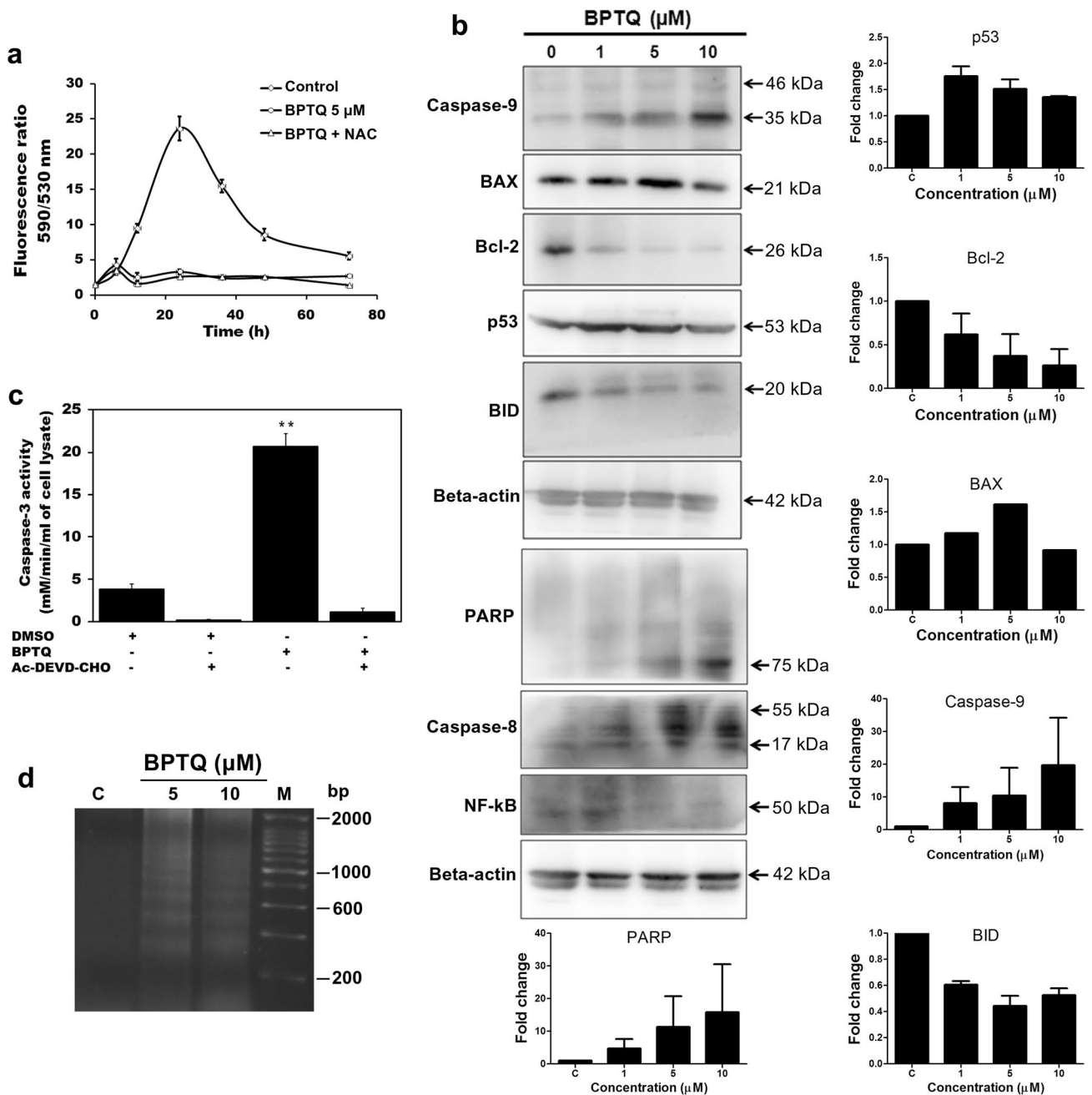


Fig. 5 BPTQ induces mitochondria-mediated apoptosis in leukemia cells. **a** BPTQ decreases the mitochondrial membrane potential without generating ROS. MOLT-4 cells were treated with BPTQ for different time intervals and then labeled with 10 μ M JC-1. Cells were washed, and fluorescence was measured. The ratio of the reading at 590 to 530 nm was considered as the relative $\Delta\psi_m$ value. NAC, N-acetyl cysteine. **b** Effect of BPTQ treatment on the expression of apoptotic proteins. Protein lysates were prepared from control and treated MOLT-4 cells and subjected to immunoblot analysis with respective antibodies mentioned. Data were presented as bar chart. β -Actin was used as loading control. **c** BPTQ increases caspase-3

expression. MOLT-4 cells were treated with 5 μ M BPTQ for 48 h before harvesting for colorimetric caspase-3 activity assay using DEVD-*p*-nitroaniline as substrate. Values were expressed as concentration of pNA formed per min per ml of cell lysate. *Ac-DEVD-CHO* represents a caspase-3 inhibitor acetyl-Asp-Glu-Val-Asp-al. **d** DNA fragmentation in MOLT-4 cells upon BPTQ treatment. Cells were treated with BPTQ for the 48 h, and DNA was prepared and then separated on 1.5 % agarose gel. *C* represents DMSO-treated control. *M* denotes molecular weight marker of 200-bp ladder. Mean \pm SEM are shown (* p < 0.05, ** p < 0.01)

Further, the expression of caspase-9, an initiator caspase of the intrinsic apoptotic pathway, was analyzed. A significant increase in the cleavage of caspase-9 was observed, confirming the intrinsic pathway. It is well known that poly (ADP-ribose) polymerase (PARP) is one of the substrates of caspase-3, the central executioner of apoptosis. The treatment of BPTQ led to the cleavage of PARP, as shown by the accumulation of cleaved product. Interestingly, the activation of caspase-8 was also observed, suggesting the involvement of the extrinsic apoptotic pathway in the cell death induced by BPTQ. These results strongly argue that cells treated with BPTQ undergo apoptosis.

Chromatin condensation and oligonucleosomal DNA fragmentation are the nuclear hallmarks of apoptosis. These phenomena were observed late during apoptosis following activation of caspases and cleavage of substrates. To analyze the involvement of BPTQ in apoptotic DNA fragmentation, DNA was prepared from MOLT-4 cells and performed agarose gel electrophoresis. Figure 5d shows DNA fragmentation in cells treated with BPTQ, demonstrated by the formation of the DNA ladder, confirming the induction of cell death by apoptosis.

Discussion

Currently, DNA and its associated processes have been recognized as potential targets for several chemotherapeutic agents. Active research and extensive investigations have developed many novel DNA-binding therapeutic molecules possessing powerful antitumor activity. As a result of such investigations, many of the anticancer regimens include a compound that binds to DNA. The purpose of this study was to examine the DNA binding and corresponding in vitro anticancer activity of BPTQ, a novel quinoline derivative. Our experimental findings clearly showed that the BPTQ is an effective intercalator of DNA. The evidence is based on the spectral (UV–visible, fluorescence, and CD), melting temperature, topological, and computational docking studies. Spectroscopic results are in agreement with an intercalation of the ellipticine, and other well-known intercalators reported earlier. First, the hypochromism and the association constants of BPTQ calculated from UV–visible absorption and fluorescence studies were of the same order to that of ellipticine [38]. The presence of an isosbestic point suggests that there is only one mode of binding. The strong quenching in the fluorescence of BPTQ indicates that the aromatic heterocyclic ring is engaged in stacking interactions with DNA. Second, the addition of BPTQ stabilizes the duplex as suggested by an increase in the midpoint denaturation temperature (T_m) of DNA. Third, titration of DNA with the BPTQ led to a change in the helical as well as the

base stack region. Considerable changes observed in the ellipticity are indicative of the intercalative nature of the BPTQ. Finally, molecular modeling and docking studies showed that BPTQ intercalates into DNA by base stacking between the d(GpC)-d(CpG) site of the duplex. Many of the intercalators such as actinomycin D, daunomycin, and ellipticine are known to possess selective specificity toward G-C sequence [20, 39]. Similar specificity was also observed for BPTQ, as judged by its increased level of binding to poly[d(G-C)] (100 % GC) DNA relative to that to calf thymus (42 % GC) and *C. perfringens* (28 % GC) DNA. Hence, by all these, it is clearly evident that BPTQ is a typical intercalator of DNA.

On confirming the DNA-binding ability, the potentiality of BPTQ at the cellular level to induce cancer cell death was elucidated. Apoptosis is a continually occurring, complicated process of regulated destruction of a cell that maintains the homeostatic cellular balance in a normal animal [40, 41]. Failing to trigger apoptotic cell death may lead to the development of neoplasia [42]. Therefore, induction of apoptosis was considered as criteria for screening of a new cancer chemotherapy agent and most chemotherapeutic drugs induce apoptosis in malignant cells [42, 43].

A panel of eight cell lines was selected to study the antiproliferative effect of BPTQ. Our investigations showed that BPTQ possesses potent cytotoxicity against all the cell lines tested and significantly reduced the number of cells upon treatment. The similar dose–response curve was observed for BPTQ against different cancer types, and the extent of anticancer ability was more than the parental APTQ [19]. As leukemia cells were more sensitive to BPTQ, it was used for the elucidation of mechanisms of cell death. BPTQ being the intercalator of DNA, we expect the DNA-associated processes as its target. Hence, the effect of the test molecule on cell cycle progression was evaluated. Interestingly, considerable S and G2 M arrest was observed upon treatment, which was in agreement with the earlier reports of well-known intercalators [44, 45].

Such arrest often leads to apoptosis of cells, supported by a dose-dependent increase in population of annexin V-positive cells upon BPTQ treatment. This was further evidenced by some of the hallmarks of apoptosis observed in the present study. Opening of the mitochondrial permeability transition pore, a putative highly regulated ion channel located between the inner and outer mitochondrial membrane is associated with mitochondria-mediated apoptotic cell death processes [46]. Bcl-2 family proteins are the antiapoptotic signals which induce such mitochondrial dysfunction. Our studies showed that BPTQ induces apoptosis in human leukemia cells by increasing the Bax:Bcl-2 ratio and thereby suppressing mitochondrial membrane potential. Activation of the caspases is the hallmark of

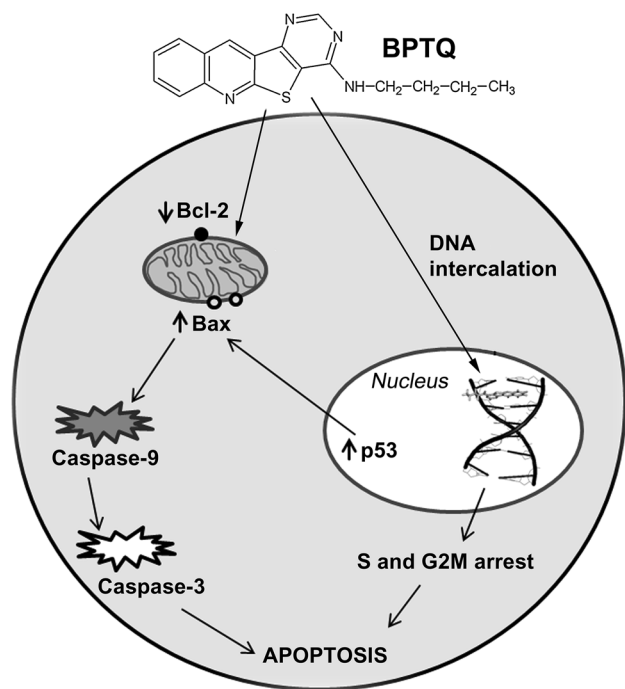


Fig. 6 Proposed model for the mechanism of BPTQ-induced apoptosis in leukemia cells

apoptosis [47]. The activation of both initiator (caspase-9) and executioner (caspase-3) caspases was observed upon BPTQ treatment. Cleavage of one of the substrates of caspase-3, PARP, was also noted, which corroborates that the mode of cell death is by apoptosis. The definitive indication of whether cells are undergoing apoptosis or necrosis is DNA laddering [42]. Internucleosomal excision was observed after the treatment with BPTQ. This DNA fragmentation event indicates the point of no return for a dying cell as cleavage of genomic DNA by endogenous endonucleases during apoptosis is an irreversible event that commits a cell to die [42].

Based on these results, we would conclude that BPTQ is a typical intercalator of DNA with effective cytotoxicity against the cancer cells. Mode of cell death was elucidated to be mitochondria-mediated apoptosis. The following model for BPTQ is suggested. (1) BPTQ intercalates into DNA; (2) arrests cells at S and G2/M phase; and (3) induces mitochondria-mediated apoptosis (Fig. 6).

Acknowledgments This work was supported by grant BT/PR10513/BRB/10/618/2008 to G. M. A. from Department of Biotechnology (DBT), Ministry of Science and Technology, Government of India (New Delhi). We are grateful to S. R. Inamdar for providing critical reagents; K. S. Rachana and M. S. Manu for critical reading; and P. Kondaiah, H. N. Kiran Kumar, and members of S. C. R. laboratory for help. FACS and confocal facilities of IISc, and FACS facility of C-CAMP, NCBS are also acknowledged. H. G. R was supported by DBT (India). We also thank Chethan Kumar for his assistance in docking studies.

Conflict of interest The authors declare no conflicts of interest.

References

- Sadikovic B, Al-Romaih K, Squire JA, Zielenska M (2008) Cause and consequences of genetic and epigenetic alterations in human cancer. *Curr Genomics* 9:394–408
- Robison K (2010) Application of second-generation sequencing to cancer genomics. *Brief Bioinform* 11:524–534
- Shahabuddin MS, Nambiar M, Choudhary B, Advirao GM, Raghavan SC (2010) A novel DNA intercalator, butylamino-pyrimido[4',5':4,5]selenolo(2,3-b)quinoline, induces cell cycle arrest and apoptosis in leukemic cells. *Invest New Drugs* 28:35–48
- Kastan MB, Bartek J (2004) Cell-cycle checkpoints and cancer. *Nature* 432:316–323
- Hurley LH (2002) DNA and its associated processes as targets for cancer therapy. *Nat Rev Cancer* 2:188–200
- Martínez R, Chacón-García L (2005) The search of DNA-intercalators as antitumoral drugs: what it worked and what did not work. *Curr Med Chem* 12:127–151
- Thurston DE (1999) Nucleic acid targeting: therapeutic strategies for the 21st century. *Br J Cancer* 80:65–85
- Li S, Cooper VR, Thonhauser T, Lundqvist BI, Langreth DC (2009) Stacking interactions and DNA intercalation. *J Phys Chem B* 113:11166–11172
- Nitiss JL (2009) Targeting DNA topoisomerase II in cancer chemotherapy. *Nat Rev Cancer* 9:338–350
- Park E-J, Kwon H-K, Choi Y-M, Shin H-J, Choi S (2012) Doxorubicin induces cytotoxicity through upregulation of per-dependent ATF3. *PLoS One* 7:e44990
- Khan SN, Lal SK, Kumar P, Khan AU (2010) Effect of mitoxantrone on proliferation dynamics and cell-cycle progression. *Biosci Rep* 30:375–381
- Kuo P-L, Hsu Y-L, Chang C-H, Lin C-C (2005) The mechanism of ellipticine-induced apoptosis and cell cycle arrest in human breast MCF-7 cancer cells. *Cancer Lett* 223:293–301
- Lafayette EA, Vitalino de Almeida SM, Pitta MGDR, Carneiro Beltrão EI, da Silva TG, Olímpio de Moura R, Pitta IDR, de Carvalho LB, de Lima MDCA (2013) Synthesis, DNA binding and topoisomerase I inhibition activity of thiazacridine and imidazacridine derivatives. *Molecules* 18:15035–15050
- Seo J, Lee HS, Lee M, Kim M, Shin C-G (2004) DA-125, a new antitumor agent, inhibits topoisomerase II as topoisomerase poison and DNA intercalator simultaneously. *Arch Pharm Res* 27:77–82
- Prajapati SM, Patel KD, Vekariya RH, Panchal SN, Patel HD (2014) Recent advances in the synthesis of quinolines: a review. *RSC Adv* 4:24463–24476
- Solomon VR, Lee H (2011) Quinoline as a privileged scaffold in cancer drug discovery. *Curr Med Chem* 18:1488–1508
- Shenoy S, Vasania VS, Gopal M, Mehta A (2007) 8-Methyl-4-(3-diethylaminopropylamino) pyrimido [4',5':4,5] thieno (2,3-b) quinoline (MDPTQ), a quinoline derivate that causes ROS-mediated apoptosis in leukemia cell lines. *Toxicol Appl Pharmacol* 222:80–88
- Shahabuddin MS, Gopal M, Raghavan SC (2009) Intercalating, cytotoxic, antitumour activity of 8-chloro and 4-morpholinopyrimido [4',5':4,5]thieno(2,3-b)quinolines. *J Photochem Photobiol B* 94:13–19
- Gopal M, Shenoy S, Doddamani L (2003) Antitumor activity of 4-amino and 8-methyl-4-(3diethylamino propylamino)pyrimido[4',5':4,5]thieno (2,3-b) quinolines. *J Photochem Photobiol B Biol* 72:69–78

20. Ren J, Chaires JB (1999) Sequence and structural selectivity of nucleic acid binding ligands. *Biochemistry* 38:16067–16075
21. Raj TT, Ambekar SY (1988) Synthesis of 4-amino pyrimido [4',5':4,5] thieno (2,3-b) quinolines. *J Chem Eng Data* 33:530–531
22. Benesi HA, Hildebrand JH (1949) A spectrophotometric investigation of the interaction of iodine with aromatic hydrocarbons. *J Am Chem Soc* 71:2703–2707
23. Huo D, Yang L, Hou C, Fa H, Luo X, Lu Y, Zheng X, Yang J, Yang L (2009) Molecular interactions of monosulfonate tetraphenylporphyrin (TPPS1) and meso-tetra(4-sulfonatophenyl) porphyrin (TPPS) with dimethyl methylphosphonate (DMMP). *Spectrochim Acta A Mol Biomol Spectrosc* 74:336–343
24. Cao Y, He XW (1998) Studies of interaction between safranin T and double helix DNA by spectral methods. *Spectrochim Acta A Mol Biomol Spectrosc* 54A:883–892
25. Tu LC, Chen C-S, Hsiao I-C, Chen J-W, Lin C-H, Shen Y-C, Yeh SF (2005) The beta-carboline analog Mana-Hox causes mitotic aberration by interacting with DNA. *Chem Biol* 12:1317–1324
26. Canals A, Purciolas M, Aymamí J, Coll M (2005) The anticancer agent ellipticine unwinds DNA by intercalative binding in an orientation parallel to base pairs. *Acta Crystallogr D Biol Crystallogr* 61:1009–1012
27. Ritchie DW, Kemp GJ (2000) Protein docking using spherical polar Fourier correlations. *Proteins* 39:178–194
28. Hegde M, Karki SS, Thomas E, Kumar S, Panjamurthy K, Ranganatha SR, Rangappa KS, Choudhary B, Raghavan SC (2012) Novel levamisole derivative induces extrinsic pathway of apoptosis in cancer cells and inhibits tumor progression in mice. *PLoS One* 7:e43632
29. Kavitha CV, Nambiar M, Ananda Kumar CS, Choudhary B, Muniyappa K, Rangappa KS, Raghavan SC (2009) Novel derivatives of spirohydantoin induce growth inhibition followed by apoptosis in leukemia cells. *Biochem Pharmacol* 77:348–363
30. Zhou N, Xiao H, Li T-K, Nur-E-Kamal A, Liu LF (2003) DNA damage-mediated apoptosis induced by selenium compounds. *J Biol Chem* 278:29532–29537
31. Srivastava M, Nambiar M, Sharma S, Karki SS, Goldsmith G, Hegde M, Kumar S, Pandey M, Singh RK, Ray P, Natarajan R, Kelkar M, De A, Choudhary B, Raghavan SC (2012) An inhibitor of nonhomologous end-joining abrogates double-strand break repair and impedes cancer progression. *Cell* 151:1474–1487
32. Zhou C, Wu Y, Yang P (2010) Synthesis, characterization, and studies on DNA binding of the complex Fe(Sal2dienNO₃, H₂O). *Biochem (Mosc)* 75:505–512
33. Garrett RH, Grisham CM (2010) *Biochemistry*. Cengage Learning, Boston
34. Piantanida I, Palm BS, Zinić M, Schneider H-J (2001) A new 4,9-diazapyrenium intercalator for single- and double-stranded nucleic acids: distinct differences from related diazapyrenium compounds and ethidium bromide. *J Chem Soc Perkin Trans 2*:1808–1816
35. Amutha R, Subramanian V, Nair BU (2001) Interaction of benzidine with DNA: experimental and modelling studies. *Chem Phys Lett* 344:40–48
36. Penninger JM, Kroemer G (2003) Mitochondria, AIF and caspases—rivaling for cell death execution. *Nat Cell Biol* 5:97–99
37. Yip KW, Reed JC (2008) Bcl-2 family proteins and cancer. *Oncogene* 27:6398–6406
38. Kohn KW, Waring MJ, Glaubiger D, Friedman CA (1975) Intercalative binding of ellipticine to DNA. *Cancer Res* 35:71–76
39. Lo Y-S, Tseng W-H, Chuang C-Y, Hou M-H (2013) The structural basis of actinomycin D-binding induces nucleotide flipping out, a sharp bend and a left-handed twist in CGG triplet repeats. *Nucleic Acids Res* 41:4284–4294
40. Hengartner MO (2000) The biochemistry of apoptosis. *Nature* 407:770–776
41. Gavrilescu LC, Denkers EY (2003) Apoptosis and the balance of homeostatic and pathologic responses to protozoan infection. *Infect Immun* 71:6109–6115
42. Cheah YH, Nordin FJ, Sarip R, Tee TT, Azimahtol HLP, Sirat HM, Rashid BAA, Abdullah NR, Ismail Z (2009) Combined xanthorhizol-curcumin exhibits synergistic growth inhibitory activity via apoptosis induction in human breast cancer cells MDA-MB-231. *Cancer Cell Int* 9:1
43. Fleischer A, Ghadiri A, Dessauge F, Duhamel M, Rebollo MP, Alvarez-Franco F, Rebollo A (2006) Modulating apoptosis as a target for effective therapy. *Mol Immunol* 43:1065–1079
44. Ralph RK, Marshall B, Darkin S (1982) Anti-cancer drugs which intercalate into DNA: how do they act? *Trends Biochem Sci* 8:212–214
45. Wu MH, Yung BY (1994) Cell cycle phase-dependent cytotoxicity of actinomycin D in HeLa cells. *Eur J Pharmacol* 270:203–212
46. Kroemer G, Galluzzi L, Brenner C (2007) Mitochondrial membrane permeabilization in cell death. *Physiol Rev* 87:99–163
47. Thornberry NA, Lazebnik Y (1998) Caspases: enemies within. *Science* 281:1312–1316